Salpeter[11] has assumed that Γ is about 0.1 ev, which gives a value of $S=0.016$ kev-barn for this reaction. This theoretical estimate appears to be too small by about a factor of 100. From the present experiment the best experimental estimate of S (for S a constant) is 1.6 kev-barns. On the basis of a more refined expression[8] for S, one expects S to vary with the bombarding energy according to $S=S_0(1-\alpha E_\alpha)$. In Fig. 5, S has been plotted as a function of the bombarding energy (note different ordinates for the two reactions). It may be seen that for both reactions S appears to vary in a linear manner for low bombarding energies and departs from this line at higher energies. In the above expression it has been assumed that only s-wave α particles contribute to the reaction; thus this departure of the cross-section factor from a straight line at higher bombarding energies may be due to the onset of p-wave α-particle contributions. A reasonable fit to the experimental data is obtained when S_0 equals 0.12 kev-barn and $\alpha=0.00051$ kev^{-1} for the $H^3(\alpha,\gamma)Li^7$ reaction, and when $S_0=2.8$ kev-barns and $\alpha=0.00055$ kev^{-1} for the $He^3(\alpha,\gamma)Be^7$ reaction.

On the basis of these estimates of S for the $He^3(\alpha,\gamma)Be^7$ reaction and the calculations of Cameron[1,3] and Fowler,[2] it appears that chain (2) or (3) could compete very favorably with chain (1) at temperatures above 10×10^6 °K.

[11] E. E. Salpeter, Phys. Rev. 88, 552 (1952).

From the spectra of γ rays taken with the 3-in. diam by 3-in. NaI crystal it is estimated that at a bombarding energy of 1320 kev about 50% of the time both reactions proceed through the first excited states, that is the 478 kev state of Li^7 and 431 kev state of Be^7. In the present experiment it was difficult to estimate how the branching ratio changed with energy; since with the 5-in. diam by 3-in. NaI crystal used to measure the yield curves there was a large probability of stopping both γ rays from the cascade.

Riley[12] has found a cross section of 0.2 μb/sterad at 90° for the $H^3(\alpha,\gamma)Li^7$ reaction at 1640 kev and a branching ratio of 5 to 2 for the ground state to first excited state transitions. On the basis of the combined uncertainties this is in reasonable agreement with the present work.

ACKNOWLEDGMENTS

The authors wish to thank Dr. W. A. Fowler of the California Institute of Technology and Dr. A. G. W. Cameron of the Chalk River Project for their helpful and encouraging correspondence. In addition the authors wish to express their gratitude to Dr. M. M. Shapiro for his encouragement of this experiment.

[12] Riley, Warren, and Griffiths, Bull. Am. Phys. Soc. Ser. II, 3, 330 (1958).

PHYSICAL REVIEW VOLUME 113, NUMBER 6 MARCH 15, 1959

Phase-Shift Analysis of Proton-Proton Scattering Experiments below 40 Mev*†

MALCOLM H. MACGREGOR
Radiation Laboratory, University of California, Livermore, California
(Received October 27, 1958)

A phase-shift analysis has been made of p-p angular distribution measurements at 1.855, 4.203, 9.68, 9.73, 18.2, 19.8, 31.8, and 39.4 Mev. At 1.855 Mev, Coulomb effects plus the nuclear S-wave phase shift are sufficient to give agreement within experimental errors. At 10 Mev, S-, P-, and D-wave effects are apparent. At 40 Mev, F-wave components are also necessary. With the aid of the Clementel-Villi parametrization method, it has been possible to determine all of the least-squares fits to the angular distribution data in the S, P, D approximation. Polarization measurements and potential model calculations can be used to further restrict the allowable phase-shift sets. It is shown that angular distribution measurements with an accuracy of 0.1% would not lead to a unique set of phase shifts. Both double- and triple-scattering experiments are necessary in order to remove the ambiguity.

I. INTRODUCTION

THE spin-space scattering matrix for p-p elastic scattering contains, as is well known, five independent complex amplitudes. Puzikov, Ryndin, and Smorodinsky[1] have shown that, in view of the unitarity conditions on the elastic scattering matrix, only five independent experiments are necessary to specify the matrix. As an example of a set of five such experiments, they list angular distribution cross section, polarization, normal component of the polarization correlation tensor, and normal components of the triple scattering tensor (depolarization) for each of the protons participating in

* This work was performed under the auspices of the U. S. Atomic Energy Commission.

† Preliminary accounts of this work were presented at the 1958 Cornell meeting of the American Physical Society [Bull. Am. Phys. Soc. Ser. II, 3, 268 (1958)], and at the Congrès International de Physique Nucléaire in Paris, France, July, 1958; published in Compt. Rend. Congrès intern. Phys. Nucleaire, Dunod, 92 Rue Bonaparte, Paris.

[1] Puzikov, Ryndin, and Smorodinsky, Nuclear Phys. 3, 436 (1957).

TABLE I. Characteristics of the four types of P-wave solutions corresponding to each pair of S and D waves.[a]

Solution type	$^3P_0$	$^3P_1$	$^3P_2$	$P(45°)$
I	$M+$	$M-$	$S+$	$+$
II	$L+$	$S-$	$S-$	$-$
III	$L-$	$S+$	$S+$	$+$
IV	$M-$	$M+$	$S-$	$-$

[a] The P-wave splitting varies somewhat as S and D are changed. Table I is most valid for the (small) D-wave values predicted by nuclear potential models. In the table, L, M, and S stand for large, medium, and small (relative to each other), and $+$ and $-$ give the sign of the phase shift. The column headed $P(45°)$ gives the sign of the polarization at a center-of-mass scattering angle of 45°.

the second scattering. This set of experiments has the virtues that all scattering measurements are in a plane and that no magnetic fields are necessary.

The present paper is an analysis of p-p scattering experiments below 40 Mev. At low energies only a few partial waves are expected to be important in the nuclear scattering, a fact that simplifies the phase-shift analysis. Unfortunately, the only accurate measurements in this energy range are angular distribution measurements. Hence the present paper is primarily a study of the restrictions imposed on phase-shift solutions by the single requirement that a good least-squares fit be obtained to the angular distribution. When the analysis was carried out using $^1S_0$, $^3P_0$, $^3P_1$, $^3P_2$ and $^1D_2$ nuclear phase shifts, it was discovered (not surprisingly) that a semi-infinite region can be described in the S–D plane inside of which equally good fits to the angular distribution are obtained, and that for each S–D pair there are four sets of P waves that give equally good fits. It is shown in Sec. IV that angular distribution measurements accurate to 0.1% would not eliminate the fourfold semi-infinite continua of solution sets. The determination of a unique phase-shift set in the S, P, D approximation requires both double- and triple-scattering experiments.

The characteristics of the four sets of P-wave solutions corresponding to an S–D pair (in the S, P, D approximation) are described in Table I. In general, sets I and III give positive polarizations, and II and IV give negative polarizations. An extrapolation of high-energy polarization measurements (see Sec. XII) shows a positive polarization, which indicates solutions of types I and III. Most nuclear potential model calculations (see Secs. XIII–XV) give a positive $^3P_0$, which would rule out III. However, Feshbach and Lomon[2] favor a large negative $^3P_0$ corresponding to type III. Hence it is difficult at present to decide conclusively which type of solution continuum is the correct one, let alone being able to extract a unique set of phase shifts from the continuum (that is, being able to assign definite values to S and D).

Precise low-energy polarization measurements will be difficult to carry out, since the polarization below 40 Mev is expected to be very small—less than 1%. Triple-scattering experiments sound even more difficult. However, the triple-scattering parameters are fairly large even at low energies (see Sec. XII). Hence experimenters who are considering low energy polarization measurements should also consider the feasibility of some of the triple-scattering measurements. The advent of polarized proton ion sources will be a boon to workers in this field.

In the present paper, Sec. II summarizes the experimental data, Secs. III–V show how many partial waves are necessary at each energy, Secs. VI–X give the detailed phase-shift analyses of the data, Sec. XI discusses error matrix calculations of the uncertainties in the phase shifts, Sec. XII covers double- and triple-scattering experiments, Secs. XIII–XV discuss the prediction of phase shifts by means of nuclear potential models, and Sec. XVI is the conclusion.

II. p-p ANGULAR DISTRIBUTION DATA

In precise phase-shift analyses, it is important that the experimental data be fully corrected. Since the present work includes analyses of data that have not yet been published, as well as cases where additional corrections were applied to data already published, it seems worthwhile to summarize the data and to discuss the corrections that have or have not been applied.

Table II contains a summary of the data[3–9] used in the present analyses. In connection with Table II, the following comments on the p-p data should be noted:

1.855 Mev.—The original Wisconsin data (first part of reference 3) have been remeasured, since the geometrical corrections were found to be incorrect. Table II gives newer data. These data have been corrected for relativistic effects and for vacuum polarization effects.[10] As this paper was being prepared for press, final data were received from Knecht. The data differ slightly from the values given in Table II, but not enough to appreciably alter the results of the present work. The reader is referred to a forthcoming article by Knecht, Messelt, Berners, and Northcliffe[11] for the latest 1.855-Mev data.

4.203 Mev.—The original data[3] contain the same geometrical errors as mentioned above for the 1.855-Mev case. The data in Table II have *not* been corrected for these errors. However, since the correction amounts to only 0.5% in cross section at most, and is considerably

[2] H. Feshbach and E. Lomon, Phys. Rev. **102**, 891 (1956).

[3] Worthington, McGruer, and Findley, Phys. Rev. **90**, 899 (1953); Knecht, Messelt, Berners, and Northcliffe, Bull. Am. Phys. Soc. Ser. II, **3**, 203 (1958); D. J. Knecht (private communication).

[4] L. H. Johnston and D. E. Young, Bull. Am. Phys. Soc. Ser. II, **3**, 50 (1958); L. H. Johnston (private communication).

[5] B. Cork and W. Hartsough, Phys. Rev. **94**, 1300 (1954).

[6] J. L. Yntema and M. G. White, Phys. Rev. **95**, 1226 (1954).

[7] Burkig, Schrank, and Richardson, Phys. Rev. **100**, 1805 (1955); Phys. Rev. **113**, 290 (1959).

[8] Cork, Johnston, and Richman, Phys. Rev. **79**, 71 (1950).

[9] L. H. Johnston and D. A. Swenson, Phys. Rev. **111**, 212 (1958).

[10] L. Durand, III, Phys. Rev. **108**, 1597 (1957).

[11] Knecht, Messelt, Berners, and Northcliffe, Phys. Rev. (to be published).

TABLE II. Summary of p-p angular distribution data used in the present analysis. (Proton bombarding energy is in lab system, Mev.)

1.855[a]		4.203[a]		9.68[b]		9.73[c]		18.24[d]		19.8[e]		31.8[f]		39.40[g]	
$\theta_{c.m.}$[h]	$\sigma(\theta)_{c.m.}$[i]	$\theta_{c.m.}$	$\sigma(\theta)_{c.m.}$	$\theta_{c.m.}$	$\sigma(\theta)_{c.m.}$	$\theta_{c.m.}$	$\sigma(\theta)_{c.m.}$	$\theta_{c.m.}$	$\sigma(\theta)_{c.m.}$	$\theta_{c.m.}$	$\sigma(\theta)_{c.m.}$	$\theta_{c.m.}$	$\sigma(\theta)_{c.m.}$	$\theta_{c.m.}$	$\sigma(\theta)_{c.m.}$
12.0059	11 082.7[j]			10.026	847.7 ±25.8									8.083	103.8 ±4.26
14.0068	5780.8[j]			12.031	401.0 ± 8.3					14.07	59.10±1.5			10.10	40.85±0.74
	5755.1[k]			14.035	218.9 ± 3.5									12.12	20.63±0.23
16.0077	3263.1[j]	16.018	637.65±7.14	16.040	138.2 ± 1.3					16.08	37.72±1.0			14.14	13.50±0.12
	3248.1[k]									18.09	29.51±0.7			16.17	10.87±0.09
20.0096	1254.8[j]									20.10	25.84±0.7			18.19	10.01±0.08
	1249.9[k]			20.050	75.49± 0.72									20.21	9.79±0.08
	1247.7[l]									22.11	24.06±0.6			22.23	9.85±0.08
24.0115	591.13[k]	25.027	153.11±0.694	24.059	58.27± 0.55					24.12	23.18±0.6			24.24	9.94±0.08
	591.02[l]			28.068	53.57± 0.51	27.67	55.69±0.50			26.13	22.39±0.6	27.52	12.94±0.16		
30.0140	274.64[k]	30.032	118.32±0.380					30.14	24.79±0.25	30.15	23.19±0.6			30.30	10.52±0.08
	274.83[l]			32.077	51.93± 0.49										
35.0161	194.92[l]	35.036	107.93±0.379	36.086	50.97± 0.48	40.41	52.26±0.43	36.16	25.78±0.26	36.18	23.40±0.6				
40.0182	166.14[l]	40.041	106.31±0.320	40.095	51.52± 0.49	49.94	53.71±0.54	40.18	26.30±0.21	40.19	23.71±0.6	40.04	13.10±0.14	40.38	10.86±0.09
50.0213	155.20[l]	50.049	108.06±0.346	50.114	53.00± 0.50	59.77	54.92±0.49	50.21	27.10±0.19	50.23	24.54±0.6	52.76	13.88±0.17	56.50	11.13±0.09
60.0244	158.84[l]	60.055	111.03±0.366	60.129	53.88± 0.51	60.28	55.24±0.60	60.24	27.29±0.16	60.26	23.88±0.6	64.98	13.95±0.20		
70.0259	163.14[l]	70.060	113.21±0.328	70.139	53.97± 0.51	68.48	54.74±0.49	70.26	27.38±0.14	70.28	24.51±0.6			70.56	11.17±0.09
80.0274	166.04[l]	80.063	114.13±0.331	80.145	54.28± 0.52	79.88	53.86±0.47	80.27	27.25±0.14	80.29	24.26±0.6	77.90	14.00±0.15	80.58	11.16±0.09
		90.065	114.32±0.354	90.148	54.49± 0.52	90.98	56.11±0.51	90.28	27.32±0.14	90.30	24.30±0.6	90.02	14.30±0.15	90.60	11.16±0.09

[a] See reference 3. *Note added in proof.*—For final values at 1.855 Mev, see D. Knecht, thesis, University of Wisconsin, 1958 (unpublished), and reference 11. [b] See reference 4. [c] See reference 5. [d] See reference 6. [e] See reference 7. [f] See reference 8. [g] See reference 9. [h] Center-of-mass scattering angle in degrees. [i] Differential scattering cross section in c.m. system, mb/sterad. [j] 1-mm defining slits. [k] 2-mm defining slits. [l] 4-mm defining slits.

less than this at large scattering angles, the phase shift values calculated from these data will be very close to the true values. The data have been corrected for relativistic angle and cross-section transformation and for vacuum polarization effects. The discussion in Sec. VI indicates the sensitivity of the calculated phase shifts to small changes in the angular distribution data.

9.68 Mev.—Johnston and Young at Minnesota[4] have measured the p-p angular distribution at 26 different scattering angles, although only 15 angles are listed in Table II. The errors shown in Table II should be regarded as preliminary, although they are expected to be very close to the final values. The data are corrected for relativistic effects. They are *not* corrected for vacuum polarization effects, although examination of the vacuum polarization corrections at 1.855 and 4.203 Mev[10] suggests that the correction is appreciable at 10 Mev, especially at small scattering angles. Since P-wave phase shifts are important at 10 Mev (see Secs. III and VII), vacuum polarization effects are pretty well masked by nuclear scattering effects.

9.73 Mev.—The published data[5] were changed only by the addition of relativistic angle and cross-section transformation effects.

18.2 Mev.[6]—Same comments as for 9.73-Mev data, above.

19.8 Mev.[7]—The final values, with all geometrical corrections, were received from Richardson,[7] who commented that although counting statistics were good to $\pm 1\%$, the final cross sections are believed to have relative accuracies of $\pm 1.5\%$ and absolute accuracies of $\pm 2.5\%$. The principal reason for uncertainty is a possible small low energy contamination in the beam. Relativistic corrections have been applied.

31.8 Mev.[8]—Same comments as for 9.73-Mev data, above.

39.40 Mev.—Johnston and Swenson[9] have made measurements at 27 angles, although only 15 angles were used in the present analysis. The data have been corrected for all geometrical and relativistic effects.

III. S-WAVE FITS TO THE ANGULAR DISTRIBUTION DATA

The simplest assumption about low-energy p-p scattering is that only Coulomb effects and S-wave nuclear forces are important. Thus it is useful to see at what bombarding energy the higher angular momentum components of the nuclear scattering become important. For the measurements at 1.855,[3] 4.203,[3] and 9.68[4] Mev, calculations were made to find the S-phase shifts which give the smallest least-squares value M, where M is defined as

$$M=\frac{1}{n}\sum_{i=1}^{n}\left[\left(\frac{\sigma_{\mathrm{calc}}(\theta_i)-\sigma_{\mathrm{exp}}(\theta_i)}{\Delta\sigma_{\mathrm{exp}}(\theta_i)}\right)^2\right], \qquad (1)$$

and $\Delta\sigma_{\mathrm{exp}}$ is the experimental uncertainty in the measured cross section. The results are summarized in

Table III. (In all phase shift calculations the equations used were those defined, for example, in the paper by Stapp and co-workers,[12] and the phase shifts are Stapp's nuclear bar phase shifts.)

The 1.855-Mev angular data used for the S-wave fit were obtained from the data in Table II by taking simple averages over the measurements at different slit widths. As Table II shows, the small-angle cross section values thus obtained have uncertainties of a few tenths of a percent. A $^1S_0$ phase shift of $44.15\pm0.01°$ gives a fit to the data that is within 0.4% for the small angles and within about 0.1% for the large angles, as shown in Table III. This value for the S phase shift agrees with the value 44.160° obtained by Knecht.[13] (See Sec. XI for a discussion of the error calculation.) The observed deviations $E(\theta)$ shown in Table III are not particularly suggestive of P- or D-wave effects. Hence, within the present experimental uncertainties, the 1.855-Mev data indicate pure S-wave nuclear scattering.

The situation at 4 Mev is not so clear-cut. The experimental measurements listed in Table II still contain the small geometrical errors discussed in Sec. II. As Table III shows, an S, P, D fit to the data gives a slightly smaller M value than the best S fit at $^1S_0 = 53.912°$, but not significantly so.

The 9.68-Mev data reveal definite P- and D-wave effects. The least-squares sum for the best S fit is almost 3 times as large as for S, P, D fits (Table III). Furthermore the deviations, which are larger than the experimental uncertainties, indicate (constructive) P-wave interference effects in the region of the minimum (~30°), and a general asymmetry characteristic of a positive D-wave component. Extrapolation of higher energy phase shift results, and potential model calculations (Secs. XIII–XV), also indicate definite P- and D-wave contributions at 10 Mev, and small but significant P- and D-wave components at 4 Mev.

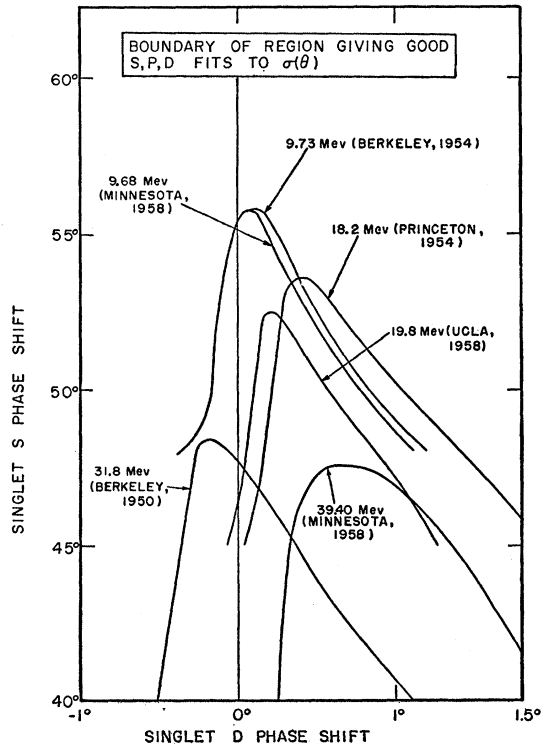

FIG. 1. Boundaries of regions inside of which good fits to the angular distributions can be obtained in the S, P, D representation.

[12] Stapp, Ypsilantis, and Metropolis, Phys. Rev. **105**, 302 (1957).

[13] D. J. Knecht (private communication).

IV. CHARACTERISTICS OF S, P, D FITS TO THE ANGULAR DISTRIBUTIONS

The S-wave approximation to p-p nuclear scattering fails even for an energy as low as 10 Mev, as shown in Sec. III. The S, P, D description of the scattering process is given in the present section. It will be shown in the next section that at 40 Mev, the S, P, D approximation fails, and F-wave components must be added.

In making a phase shift analysis of p-p scattering using nuclear S, P, and D waves, we make use of the parametrization method developed by Clementel and Villi.[14] The application of this method to measurements at 40 Mev has been described in a previous paper.[15] Clementel and Villi write the differential cross section in the form

$$\sigma(\theta)=A_0(^1S_0,^1D_2,\theta)+A_1(\theta)Z_1+A_2(\theta)Z_2+A_3(\theta)Z_3, \quad (2)$$

where Z_1, Z_2, and Z_3 are certain combinations of the $^3P_0$, $^3P_1$, and $^3P_2$ phase shifts [Eq. (2) of reference 15]. Now if values for $^1S_0$ and $^1D_2$ are chosen and the least-

TABLE III. Summary of S-wave fits to p-p angular distribution data.

Lab energy (Mev):	1.855[a]		4.203[a]		9.68[a]	
$^1S_0$ phase shift for best fit	$44.15\pm0.01°$		53.912°		56.15°	
M value for S fit[b]	···		0.267		0.82	
M value for S, P, D fit	···		0.195		0.30	
Deviation $E(\theta)$ in %:[c]						
	$\theta_{c.m.}$[d]	$D(\theta)$	$\theta_{c.m.}$	$D(\theta)$	$\theta_{c.m.}$	$D(\theta)$
	12	0.23	16	0.18	12	−0.93
	14	0.20	25	−0.16	14	−0.21
	16	0.27	30	−0.41	16	−0.99
	20	0.37	35	0.19	20	0.13
	24	0.38	40	−0.08	24	−0.48
	30	0.23	50	0.19	28	−1.93
	35	−0.07	60	0.03	32	−1.50
	40	−0.11	70	−0.14	36	0.33
	50	−0.11	80	0.05	40	0.12
	60	−0.10	90	0.19	50	−0.09
	70	0.07			60	0.19
	80	0.12			70	1.21
					80	1.28
					90	1.08

[a] See discussion of these data in Sec. II.
[b] M is the least-squares sum, see Eq. (1).
[c] $E(\theta)=[\sigma_{calc}(\theta)-\sigma_{exp}(\theta)]/\sigma_{calc}(\theta)$.
[d] Approximate center-of-mass scattering angle in degrees.

[14] Clementel, Poiani, and Villi, Nuovo cimento **2**, 352 (1955); and E. Clementel and C. Villi, Nuovo cimento **2**, 1165 (1955).

[15] H. P. Noyes and M. H. MacGregor, Phys. Rev. **111**, 223 (1958).

squares sum M [Eq. (1)] minimized, the Z's can be uniquely determined.[15] When the Z equations are solved for $^3P_0$, $^3P_1$, and $^3P_2$, it is found[14,15] that there are four sets of P waves that all give the same set of Z's, and hence the same values for $\sigma(\theta)$ and for M.

When the data of Sec. II were subjected to a phase shift analysis in the S, D, Z_1, Z_2, Z_3 representation, it was found that at 20 Mev and below, the least-squares sum M is constant for all values of S and for a whole range of D values. (For the situation at 40 Mev, see reference 15.) When the Z equations were solved for the P phase shifts, however, it was found that only certain combinations of S and D waves lead to real values for $^3P_0$, $^3P_1$, and $^3P_2$. Figure 1 gives regions in the S, D plane, for each set of data, inside of which real P values are obtained. Outside of these regions, good fits in the S, P, D approximation cannot be obtained.

A number of investigations were carried out to determine the properties of the solution regions shown in Fig. 1. Removal of the Coulomb peak from the 9.68-Mev data did not change the shape of the solution region, and changed the resulting phase shift sets only slightly. This shows that attempts to fit the Coulomb peak were not dominating the results. A series of search problems were started at random phase shift values, with the S and D phase shifts held constant. For S–D pairs lying within the solution region (Fig. 1), one or another of the Clementel-Villi P-wave solution sets was always obtained. For S–D pairs lying outside the solution region, P-wave solution sets were still obtained, but with much poorer least-squares fits to the data.

The variations in the P-wave solution sets with variations in S and D are illustrated in Figs. 2–4. Both P

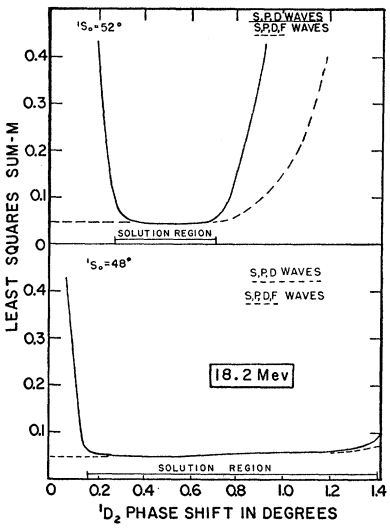

FIG. 3. Variation of the least-squares sum M with changing D phase shift, holding the S phase shift fixed. This illustrates that, with S, P, and D waves, good fits to the angular distribution are obtained only inside the solution region (Fig. 1).

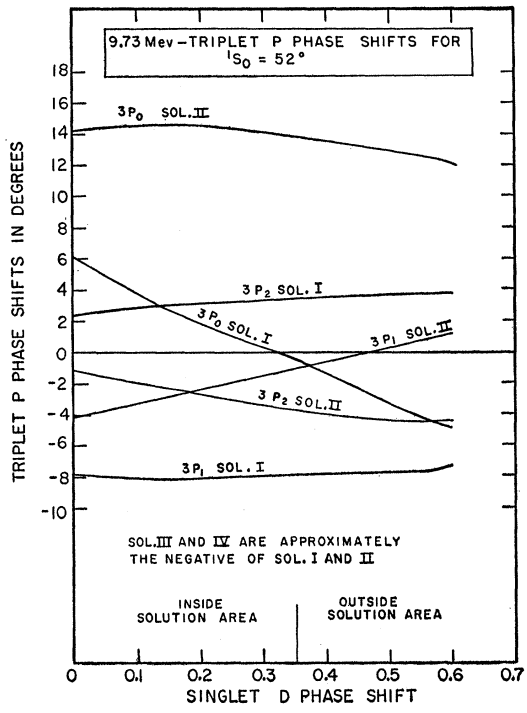

FIG. 2. Variation of P phase shifts as the D phase shift is varied, with the S phase shift held constant. The P phase shifts are smoothly varying in going across the boundary of the solution region (Fig. 1), although good fits to the angular distribution are no longer obtained outside the solution region. The solution sets are labeled according to Table I.

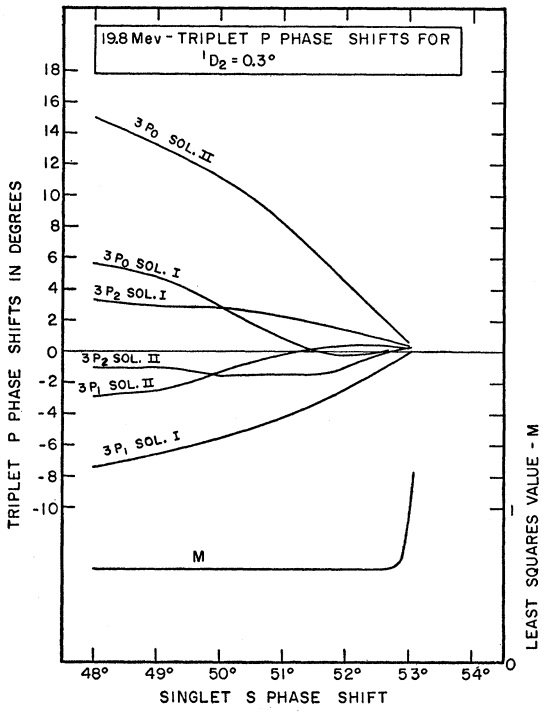

FIG. 4. Variation of P phase shift as the S phase shift is varied, with the D phase shift held constant. Above a certain value for the S phase shift, good fits to the angular distribution can no longer be obtained.

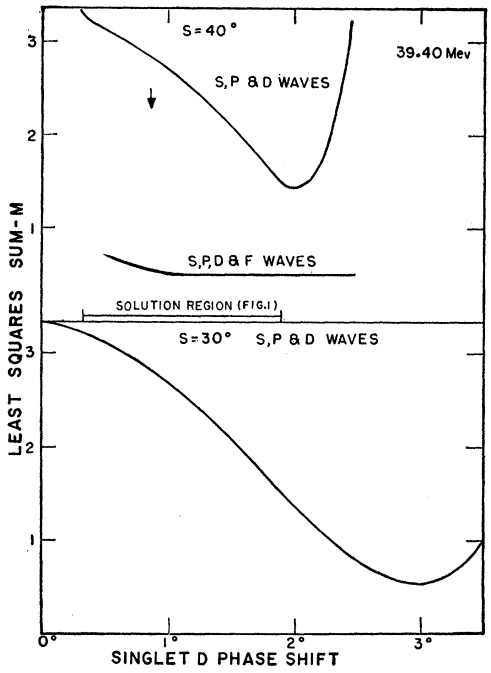

FIG. 5. Least-squares fits at 39.40 Mev. For $S=30°$ and $D=3°$, good S, P, D fits to the angular distribution (but not to the polarization) are obtained. For $S=40°$, the solution boundary effects (Fig. 1) are apparent in the S, P, D solution, and F waves are needed to give good fits to the angular distribution. The arrow indicates the probable value for the D-wave phase shift, based on nuclear potential model calculations.

and D waves have large $\cos^2\theta$ components, and for energies of 20 Mev and below, the $\cos^4\theta$ component in the angular distribution is unimportant [see the discussion of Eq. (3) in the next section]. Hence a change in the D wave can be compensated for by a suitable change in the P waves. Figure 2 shows how this works out in a particular case. Although the P-wave solutions are smooth functions of the D wave in passing across the solution region boundary (Fig. 2), the least-squares sum M rises sharply outside the solution region, as illustrated in Fig. 3. Figure 3 also shows that the addition of F waves does not improve the fit inside the solution region. (This is not true at 40 Mev, as will be shown in the next section.) F waves help somewhat in obtaining agreement outside the solution region, although the effect of crossing the boundary is still apparent.

We have shown that if the single criterion of a phase shift search is to obtain the best possible least-squares fit to an angular distribution curve, the S, P, D approximation at energies of 20 Mev and below gives four semi-infinite continua of solution sets. However, since M represents a sum over many angles, it might still be hoped that a certain portion of the angular distribution curve (for example, the interference dip) will show changes in the calculated cross sections for the different phase shift solution sets. An examination of the calculated cross sections reveals that at any one angle, the cross section value is constant to within one- or two-tenths of a percent for all solutions inside the allowed region. Hence even a very accurate angular distribution measurement will not be sufficient to eliminate any of these solution sets.

The constancy of the cross section means that a certain combination of squares of the scattering amplitudes [Eq. (4.4) in reference 1] is constant for all of the solution sets. However, the amplitudes themselves are not constant, and the polarization and triple-scattering parameters vary throughout the solution region shown in Fig. 1 and are different for solutions of the various types I–IV. Thus polarization and triple-scattering measurements will provide data to remove the phase-shift ambiguity.

V. F-WAVE EFFECTS

In the preceding section, it was shown in Fig. 3 that the addition of F waves did not improve the fit to the angular distribution in the solution region. (Since the solution regions shown in Fig. 1 contain the physically interesting ranges of S and D, any improvement in the fits outside the solution regions by the addition of F waves is of no practical importance.) Analysis of the data at 19.8-Mev yields curves similar to those shown in Fig. 3. Hence at 20 Mev and below, the angular distribution data indicate no necessity for adding F-wave components.

At 40 Mev the situation is considerably different. A solution region can be defined in the S, P, D approximation, as shown in Fig. 1. However, good fits are not obtained at all points inside the region, using only S, P, and D waves. Figure 5 shows that if a D wave of 3.1° is chosen, a fit can be obtained for S, P, and D waves that is as good as when F waves are added. However, a D wave this large means that the S wave can be no larger than 33° or the S–D set will lie outside the solution region and the good fit will no longer be obtained. This is shown in the $S=40°$ curve at the top of Fig. 5. A D wave of 3.1° is much larger than potential model calculations predict, and an S wave of 33° is much smaller than the extrapolation from low energy results indicates. Furthermore, the S, P, D solutions that give reasonable fits to the angular distribution also predict large polarizations, whereas the experimentally measured polarization at 40 Mev is small[16] (see Sec. XII). Hence any possibility of a satisfactory fit to angular distributions and polarizations at 40 Mev using only S, P, and D waves is ruled out. (These conclusions were stated in reference 15 and are included here again only for completeness).

With the search code used in the present work, the $^3P_2-{}^3F_2$ coupling parameter and $^3F_2$ phase shift could be added to the phase shift search problem. When this was done, good fits to angular distributions were obtained for reasonable values of S and D, as shown in Fig. 5.

[16] Palmeiri, Cormack, Ramsey, and Wilson, Ann. Phys. (N. Y.) 5, 299 (1958).

TABLE IV. S, P, D phase-shift solution sets at 4.203 Mev.[a]

$^1S_0$ / $^1D_2$	51° $^3P_0$	51° $^3P_1$	51° $^3P_2$	52° $^3P_0$	52° $^3P_1$	52° $^3P_2$	53° $^3P_0$	53° $^3P_1$	53° $^3P_2$	53.5° $^3P_0$	53.5° $^3P_1$	53.5° $^3P_2$	53.7° $^3P_0$	53.7° $^3P_1$	53.7° $^3P_2$
							Solution I								
0°	4.85	−6.02	2.48	4.23	−4.83	1.95	3.94	−3.18	1.10	3.74	−1.68	0.25	2.41	−1.26	0.25
0.5°	4.11	−6.09	2.66	3.14	−4.92	2.20	0.65	−3.30	1.72	−1.92	−1.65	1.26	−1.99	−0.96	0.93
0.1°	3.10	−6.13	2.85	1.55	−4.92	2.45	−0.17	−3.28	1.89	−2.44*	−1.62	1.41			
0.2°	0.43	−6.01	3.19	−0.92	−4.69	2.76	−2.03*	−3.01	2.15	−3.67*	−1.29	1.57			
0.3°	−4.50*	−4.99	3.32	−3.32*	−4.18	2.91									
							Solution II								
0°	11.81	−3.04	−0.52	9.52	−2.38	−0.50	6.27	−2.09	−0.00	4.04	−1.43	0.03	2.64	−1.10	0.11
0.05°	12.04	−2.37	−1.02	9.73	−1.68	−1.00	6.55	−0.57	−1.06	3.76	−0.67	−0.54			
0.1°	12.04	−1.69	−1.50	9.63	−0.92	−1.50	4.83	1.23	−1.91	4.24*	0.44	−1.13	3.96*	−0.25	−0.56
0.2°	11.96	−0.88	−2.00	9.17	0.16	−2.11	3.47*	2.36	−2.21	4.33*	1.02	−1.39			
0.3°	11.18*	0.33	−2.71	7.96*	1.46	−2.70									
							Solution III								
0.05°	−12.19	2.03	1.01	−9.82	1.31	1.00	−6.68	0.39	0.99	−4.64	0.70	0.50	−2.91	1.40	−0.21
							Solution IV								
0.05°	−4.77	5.96	−2.70	−3.80	4.85	−2.20	−2.30	3.39	−1.60	1.32	1.71	−1.39	1.81	1.00	−1.00

[a] The phase shifts are nuclear phase shifts in degrees. Solution sets noted with an asterisk lie outside the solution region (Fig. 2) and do not give as good fits to the angular distribution as the sets lying within the solution region.

Also, solutions were obtained which give the small polarizations required by experiment.

Since we have shown that F-wave effects are very important at 40 Mev, the question arises as to the importance of F waves at 20 Mev. Although good fits to the angular distribution data at 20 Mev are obtained using only S, P, and D waves, this does not necessarily rule out the existence of F waves. The angular distribution cross section can be written in the form

$$K^2\sigma = a + b\cos^2\theta + c\cos^4\theta + \text{Coulomb terms} + \text{Coulomb-nuclear interference terms}, \quad (3)$$

where K is the c.m. wave number and θ is the c.m. scattering angle. Now both D waves and F waves contribute to the $\cos^4\theta$ term. Hence if c is large it will not be easy to distinguish between D- and F-wave effects. On the other hand, if c is small, then the main importance of the D wave lies in its contributions to b and to the interference terms. To the extent that it contributes to b, the F wave cannot be distinguished from P-wave effects.

When the angular distributions at 20 Mev and below were analyzed in terms of Eq. (2), it was found that the $\cos^4\theta$ component is quite small. For example, at 18.2 Mev, the phase shift solution set: $S=50°$, $P_0=7.70°$, $P_1=-5.38°$, $P_2=4.18°$, $D=0.4°$, which gives an excellent fit to the angular distribution, corresponds to the values $a=0.63$, $b=0.072$, $c=0.0027$. Values at 19.8 Mev are $a=0.62$, $b=0.026$, $c=0.0027$, and at 9.68 Mev are $a=0.68$, $b=0.013$, $c=0.0002$. At 39.40 Mev, on the other hand, we have $a=0.55$, $b=-0.017$, $c=0.124$. Hence for bombarding energies of 20 Mev and below, it is reasonable to talk in terms of S, P, and D waves only, even though at 40-Mev F-wave effects are so pronounced.

VI. ANALYSIS OF 4.203-MEV DATA

The Wisconsin p-p angular distribution data at 4.203 Mev,[3,13] as shown in Table II, have been analyzed in terms of S, P, and D waves. The results are summarized in Table IV. The solution sets are continuous with respect to changes in S and D, of course, and the discrete values for S and D shown in Table IV serve to outline the nature of the solutions and can be used for interpolation if necessary. Solutions of types I and II have been mapped out in considerable detail. Solutions III and IV have P-waves that are approximately the negative of those for types II and I, respectively, and only a few solution sets are shown for these cases. Due to scaling difficulties, the Clementel-Villi parametrization method was not used to map out the solution region (Fig. 1) at 4.203 Mev, but with the aid of the search code the boundary limits could be readily identified. The solution sets noted with an asterisk lie outside the solution region and hence do not give good fits to the angular distributions. They are included here only for completeness.

As discussed in Sec. II, the 4.203-Mev data still contain small errors due to inaccurate geometrical corrections. Also, vacuum polarization[10] corrections have been applied. To see the effect of the vacuum polarization corrections on the phase-shift solution sets, consider Table V, which gives phase shift solutions obtained before vacuum polarization corrections were applied. A comparison of Tables IV and V shows that the effect of the vacuum polarization corrections is to change the phase shifts slightly. Thus unless the S phase shift is in the region where the P waves are very small ($S>53.7°$), the vacuum polarization corrections to the phase shifts at 4 Mev are not too important. Since the errors due to inaccurate geometrical corrections to the 4.203-Mev data are (coincidentally) about the same size as the vacuum polarization corrections, it follows that subse-

TABLE V. S, P, D phase-shift solution sets at 4.203 Mev with no vacuum polarization corrections applied.

$^1S_0$ / $^1D_2$	52° $^3P_0$	52° $^3P_1$	52° $^3P_2$	53° $^3P_0$	53° $^3P_1$	53° $^3P_2$
			Solution I			
0°	3.84	−4.83	1.95			
0.05°	2.89	−4.89	2.17	0.95	−3.28	1.62
0.1°	1.62	−4.91	2.39	−0.43	−3.20	1.84
			Solution II			
0°	9.36	−2.42	−0.50	6.04	−2.11	0.00
0.05°	9.58	−1.72	−1.00	6.35	−0.58	−1.06
0.1°	9.49	−0.96	−1.50	4.09	1.53	−2.00

quent improvement in the 4.203-Mev data will not materially alter the phase shifts shown in Table IV.

The uncertainties in the phase shifts shown in Table IV can be estimated by means of error matrix calculations, using the methods of Anderson *et al.*[17] (see Sec. XI). The polarizations corresponding to the phase shift solutions in Table IV were calculated and are summarized in Sec. XII.

Recently Hull and Shapiro[18] published the results of a phase-shift analysis of the 4.203-Mev p-p data in which they correctly showed that the angular distribution can be matched with solution sets having large P- and D-wave components (and hence large polarizations). A comparison of their phase-shift results with those of Table IV shows that their solutions are all of the types labeled II and III in Table IV. Furthermore, their solutions have large D values (for $S<53°$ their solutions lie outside of the solution boundary region) and hence are in regions where $^3P_0$ and $^3P_1$ have the same sign, as can be seen in Table IV. Thus their statement that the phase shift sets are characteristic of $\mathbf{L}\cdot\mathbf{S}$ splitting is somewhat misleading, since over most of the solution region this is not the case.

VII. ANALYSES OF 9.68-MEV AND 9.73-MEV DATA

Phase-shift analyses of the Minnesota 9.68-Mev data[4] and Berkeley 9.73-Mev data[5] were carried out in the same manner as described in the preceding section. Due to scaling difficulties, the 9.68-Mev data were analyzed with a 10° c.m. point omitted. Studies showed that this omission had a negligible effect on the phase shift solutions.

When only S waves are used, the lowest M values that can be obtained are $M=0.82$ at 9.68 Mev for $S=56.15°$, and $M=4.4$ at 9.73 Mev for $S=56.8°$. [The least-squares sum M is defined in Eq. (1).] When P and D waves are added, the M values drop to 0.30 and 1.9 for the 9.68-Mev and 9.73-Mev cases, respectively. Hence both sets of data show definite improvement when the higher angular momentum components are added.

As a first approximation, the M value as defined in Eq. (1) is expected to equal $(n-p)/n$, where n is the number of angles used in the fit and p is the number of parameters used in the phase shift analysis. Hence we expect $M=0.64$ for the 14-angle 9.68-Mev data and $M=0.37$ for the 8-angle 9.73-Mev data, when S, (split) P, and D waves are used. At 9.68 Mev, the M value obtained is about half of the expected value, showing that the errors quoted in Table II are somewhat conservative. At 9.73 Mev, on the other hand, the observed M value is 5 times as large as expected, showing that the experimental errors are actually larger than shown in Table II.

The results of the phase-shift search are shown in Table VI. The phase shift sets obtained at 9.68 Mev and 9.73 Mev are quite similar, although a slight shift with respect to the D wave can be observed. As stated in Sec. II, vacuum polarization effects were not included. Although a rough extrapolation indicates that the vacuum polarization correction is appreciable at 10 Mev, the effect on the phase shifts in Table VI would be slight.

VIII. ANALYSES OF 18.2-MEV AND 19.8-MEV DATA

This section includes the phase-shift analyses of the 18.2-Mev Princeton data[6] and the 19.8-Mev UCLA data.[7] The Princeton data does not include measurements at small angles, and the experimental uncertainties are very small. The UCLA data, on the other hand, does include measurements at small angles, but the quoted errors are rather large. The principal uncertainty in the UCLA data, as was mentioned in Sec. II, is a possible small low-energy contamination in the proton beam. The least-squares values expected at 18.2 and 19.8 Mev are 0.38 and 0.67, respectively, when S, P, and D waves are used. The actual values obtained were 0.05 and 0.61 for the two cases. This shows that the 18.2-Mev errors are quite conservative, while the 19.8-Mev errors are about as quoted. However, if the point at 14° is dropped from the 19.8-Mev analysis, an M value of 0.17 is obtained as compared to an expected M value of 0.64. Hence with the exception of the smallest angle, the 19.8-Mev errors are not as large as shown in Table II. A study showed that dropping the 14° point from the analysis increased the 19.8-Mev $^3P_0$ phase shift by about 10% and had smaller effects on the rest of the phase shifts. In mapping the 19.8-Mev phase shifts shown in Table VIII, all angles were used in the analysis.

The phase-shift analyses of the 18.2-Mev data and 19.8-Mev data are summarized in Tables VII and VIII, respectively. The solution sets are quite similar, although for the same P-wave splitting, the 18.2-Mev data require larger D waves than do the 19.8-Mev data. This is also borne out in the solution region boundaries shown in Fig. 1. Polarizations are summarized in Sec. XII.

[17] Anderson, Davidon, Glicksman, and Kruse, Phys. Rev. **100**, 279 (1955).
[18] M. H. Hull, Jr., and J. Shapiro, Phys. Rev. **109**, 846 (1958).

TABLE VI. S, P, D phase-shift solution sets at 9.68 and 9.73 Mev.[a]

$^1S_0$ / $^1D_2$	52°			53°			54°			55°			55.5°			55.8°			56°		
	$^3P_0$	$^3P_1$	$^3P_2$	$^3P_0$	$^3P_1$	$^3P_2$	$^3P_0$	$^3P_1$	$^3P_2$	$^3P_0$	$^3P_1$	$^3P_2$	$^3P_0$	$^3P_1$	$^3P_2$	$^3P_0$	$^3P_1$	$^3P_2$	$^3P_0$	$^3P_1$	$^3P_2$
9.68 Mev: Solution I																					
0°	8.13	−6.75	2.19	7.12	−5.82	1.85	5.97	−4.71	1.43	4.36*	−3.30	0.92	2.90*	−2.35	0.65	1.41*	−1.46	0.40	0.39*	0.21	−0.37
0.1°	6.27	−7.07	2.69	5.47	−6.11	2.31	4.36	−5.00	1.91	3.08	−3.55	1.35	1.71	−2.50	1.00	1.56	−1.68	0.58	0.71	−0.88	0.29
0.2°	4.77	−7.21	3.00	3.91	−6.23	2.64	2.83	−5.07	2.22	1.26	−3.59	1.71	−1.66	−2.10	1.40	−1.26*	−1.30	0.92	−0.41*	−1.02	0.66
0.3°	2.81	−7.27	3.33	1.66	−6.25	3.00	0.17	−5.01	2.62	−2.13*	−3.13	2.05	−2.76*	−1.88	1.54						
0.4°	1.00	−7.21	3.58	−0.43	−6.10	3.25	−2.83*	−4.48	2.81												
0.5°	−0.89	−7.03	3.76	−3.56*	−5.50	3.38	−4.72*	−3.95	2.89												
Solution II																					
0°	13.36	−3.96	−0.47	11.52	−3.36	−0.49	9.32	−2.71	−0.46	6.47*	−1.87	−0.39	4.27*	−1.52	−0.14	2.63*	−0.90	−0.18	−0.07*	0.52	−0.47
0.1°	13.85	−2.96	−1.25	11.93	−2.44	−1.18	9.68	−1.68	−1.20	6.61	−0.63	−1.21	4.57	−0.29	−0.95	2.92	−0.11	−0.67	−0.22	0.96	−0.62
0.2°	13.91	−2.07	−1.88	11.98	−1.65	−1.72	9.36	−0.49	−1.95	4.41	1.53	−2.16	3.71	0.81	−1.42	2.30*	0.70	−1.00	0.32*	0.99	−0.69
0.3°	13.70	−1.20	−2.46	11.51	−0.47	−2.47	7.13	1.65	−2.96	2.46*	2.69	−2.37	2.23*	2.01	−1.77						
0.4°	13.19	−0.29	−3.02	10.43	0.81	−3.16	4.60*	3.14	−3.31	3.56*	2.44	−2.38									
0.5°	12.72	0.39	−3.38	8.11*	2.50	−3.83															
Solution III																					
0.1°	−14.08	3.07	0.59	−12.20	2.45	0.62	−9.94	1.88	0.58	−7.03	0.88	0.64	−4.89	0.49	0.50				−0.70	−0.71	0.46
Solution IV																					
0.1°	−6.04	6.77	−3.16	−6.71	5.73	−2.27	−3.87	4.76	−2.34	−2.10	3.34	−1.81	−2.30	2.31	−1.07				−0.82	0.79	−0.40
9.73 Mev: Solution I																					
0.1°	3.79	−8.05	2.82	2.55	−7.13	2.54	1.58	−6.04	2.17	1.01	−4.67	1.73									
0.2°	1.85	−8.07	3.11	0.10	−7.03	2.83	−0.56	−5.91	2.46	−2.46	−4.29	2.00									
Solution II																					
0.1°	14.37	−3.18	−1.93	12.54	−2.64	−1.91	10.47	−2.08	−1.82	7.84	−1.19	−1.81									
0.2°	14.35	−2.31	−2.53	12.44	−1.71	−2.53	10.18	−0.97	−2.18	6.94	0.26	−2.57									

[a] The phase shifts are nuclear phase shifts in degrees. Solution sets noted with an asterisk lie outside the solution region (Fig. 2) and do not give as good fits to the angular distribution as the sets lying within the solution region.

TABLE VII. S, P, D phase-shift solutions at 18.2 Mev.[a]

$^1S_0$ / $^1D_2$	48°			49°			50°			51°			52°			53°			54°		
	$^3P_0$	$^3P_1$	$^3P_2$	$^3P_0$	$^3P_1$	$^3P_2$	$^3P_0$	$^3P_1$	$^3P_2$	$^3P_0$	$^3P_1$	$^3P_2$	$^3P_0$	$^3P_1$	$^3P_2$	$^3P_0$	$^3P_1$	$^3P_2$	$^3P_0$	$^3P_1$	$^3P_2$
Solution I																					
0°	13.85*	−6.04	2.07	12.43*	−5.46	1.67	10.69*	−4.85	1.35	8.63*	−4.12	1.04	6.09*	−3.12	0.70	1.94*	−1.09	0.08			
0.2°	13.44	−5.99	3.60	13.33*	−4.96	2.85	12.05*	−4.25	2.35	10.07*	−3.66	2.02	7.75*	−2.84	1.65	4.74*	−1.45	1.12			
0.3°	10.96	−6.67	4.42	10.58	−5.81	4.01	10.34	−4.79	3.51	9.11	−3.95	3.01	7.81*	−2.82	2.41	5.76*	−1.28	1.66			
0.4°	9.28	−6.97	4.87	8.55	−6.21	4.54	7.69	−5.38	4.18	6.77	−4.41	3.79	5.46	−3.29	3.34	3.70	−1.73	2.77	1.55*	1.55	1.54
0.6°	6.19	−7.30	5.45	5.20	−6.54	5.14	3.94	−5.70	4.81	2.71	−4.40	4.50	0.73	−3.21	4.13	−2.16*	−0.61	3.57			
0.8°	3.83	−7.20	5.99	2.55	−6.40	5.66	1.07	−5.40	5.34	−1.08	−4.07	4.95	−3.75*	−1.76	4.54	−2.53*	−0.41	4.09			
Solution II																					
0°	13.39*	−6.25	2.22	11.87*	−5.72	1.88	10.24*	−5.06	1.52	8.58*	−4.15	1.07	6.34*	−2.99	0.57	1.94*	−1.11	0.10			
0.2°	16.37	−4.59	2.25	14.00*	−4.64	2.56	11.54*	−4.50	2.54	9.84*	−3.76	2.11	7.72*	−2.85	1.66	4.74*	−1.44	1.11			
0.3°	17.86	−3.24	0.96	16.14	−3.05	1.18	14.26	−2.78	1.37	11.41	−2.95	2.16	9.42*	−2.02	1.68	6.01*	−1.16	1.54			
0.4°	18.34	−2.43	0.28	16.74	−2.10	0.38	15.01	−1.69	0.46	13.03	−1.24	0.58	10.71	−0.65	0.71	7.59	0.21	0.83			
0.6°	18.83	−1.07	−0.49	17.20	−0.63	−0.48	15.34	−0.10	−0.53	13.27	0.57	−0.50	10.52	1.55	−0.56	5.78*	3.42	−0.44			
0.8°	18.73	0.21	−1.27	16.95	0.74	−1.30	14.87	1.43	−1.36	12.24	2.42	−1.43	8.08*	4.16	−1.37	6.27*	4.09	−0.39			
Solution III																					
0.4°	−15.63	5.24	2.31	−14.03	4.91	2.23	−12.28	4.50	2.16	−10.42	3.82	2.07	−8.04	3.28	2.00	−4.87	2.46	1.93			
0.6°	−16.17	3.64	3.17	−14.55	3.15	3.15	−12.73	2.60	3.14	−10.58	1.92	3.18	−7.76	0.95	3.26	−2.73*	−0.36	3.50			
Solution IV																					
0.4°	−6.35	9.90	−1.94	−5.42	8.85	−2.04	−4.73	8.14	−1.50	−3.72	7.14	−1.16	−2.81	6.07	−0.53	−0.73	4.43	−0.12			
0.6°	−3.56	9.93	−2.82	−2.68	9.18	−2.50	−1.69	8.38	−2.11	−0.32	7.32	−1.80	1.64	5.98	−1.40	5.27*	3.65	−0.50			

[a] The phase shifts are nuclear phase shifts in degrees. Solution sets noted with an asterisk lie outside the solution region (Fig. 2) and do not give as good fits to the angular distribution as the sets lying within the solution region.

TABLE VIII. S, P, D phase-shift solutions at 19.8 Mev.[a]

$^1S_0$ / $^1D_2$	48°			49°			50°			51°			51.5°			52°			53°		
	$^3P_0$	$^3P_1$	$^3P_2$	$^3P_0$	$^3P_1$	$^3P_2$	$^3P_0$	$^3P_1$	$^3P_2$	$^3P_0$	$^3P_1$	$^3P_2$	$^3P_0$	$^3P_1$	$^3P_2$	$^3P_0$	$^3P_1$	$^3P_2$	$^3P_0$	$^3P_1$	$^3P_2$
Solution I																					
0°	10.36*	−6.37	2.00	10.73*	−4.85	1.01	9.73*	−3.51	0.32	7.41*	−2.52	0.14	5.49*	−2.30	0.39	3.67*	−1.15	0.04			
0.1°	9.05	−6.73	2.45	8.46	−5.73	1.98	7.83*	−4.52	1.38	5.25*	−3.63	1.31	4.79*	−2.62	0.80	2.55*	−1.86	0.78			
0.2°	7.35	−7.05	2.91	6.88	−6.06	2.45	5.96	−4.99	2.00	3.84	−3.86	1.73	2.86	−3.03	1.44	1.61	−1.90	1.03	0.39*	0.24	0.30
0.3°	5.06	−7.32	3.39	4.00	−6.40	3.07	2.73	−5.33	2.71	1.13	−3.94	2.24	−0.10	−2.95	1.93	−0.81*	−1.68	1.40			
0.4°	3.14	−7.40	3.71	1.95	−6.43	3.39	0.44	−5.25	3.03	−2.58	−3.36	2.54	−2.79*	−2.35	2.10	−2.03*	−1.52	1.62			
0.5°	1.42	−7.36	3.94	0.08	−6.31	3.62	−1.96	−4.91	3.23	−4.50*	−2.69	2.56	−3.46*	−2.22	2.24						
0.6°	−0.34	−7.21	4.12	−2.03	−6.01	3.78	−4.70*	−4.16	3.28	−5.52*	−2.24	2.59	−4.21	−1.89	2.28						
Solution II																					
0°	13.75*	−4.49	0.21	11.55*	−4.32	0.51	8.56*	−4.26	1.02	6.21*	−3.33	0.89	5.69*	−2.08	0.21	3.63*	−1.20	0.08			
0.1°	14.24	−3.96	−0.19	12.27	−3.67	0.00	9.59*	−3.62	0.50	7.60*	−2.37	0.08	6.07*	−1.73	−0.02	3.88*	−0.60	−0.29			
0.2°	14.43	−3.74	−0.30	12.75	−3.00	−0.50	10.78	−2.02	−0.79	8.14	−1.42	−0.61	6.40	−1.17	−0.38	4.02	−0.09	−0.57	0.41*	0.36	0.22
0.3°	14.89	−2.72	−1.10	13.03	−2.29	−1.01	10.80	−1.01	−1.48	7.93	−0.10	−1.44	5.80	0.62	−1.43	3.59*	0.77	−0.96			
0.4°	14.80	−1.39	−2.10	12.87	−0.91	−2.00	10.45	−0.10	−2.02	5.84	1.88	−2.32	5.29*	1.29	−1.68	3.13*	1.54	−1.25			
0.5°	14.59	−0.74	−2.51	12.78	−0.49	−2.22	9.11	1.38	−2.78	4.20*	2.95	−2.55	3.86*	2.39	−1.99	2.96*	1.88	−1.33			
0.6°	13.89	0.30	−3.15	11.74	0.86	−3.01	7.98*	2.31	−3.12	4.81*	2.85	−2.52	4.19*	2.46	−2.00						
Solution III																					
0.2°	−14.33	3.71	0.70	−12.55	3.17	0.69	−10.57	2.38	0.78	−7.93	1.71	0.70	−6.23	1.31	0.63	−3.85	0.43	0.70	0.43*	0.34	0.23
0.4°	−14.92	1.60	1.85	−12.92	0.93	1.89	−10.46	0.04	1.98	−5.70	−1.97	2.28	−5.25*	−0.99	1.79	−2.74*	−1.10	1.50			
Solution IV																					
0.2°	−6.92	7.29	−2.80	−5.62	6.42	−2.58	−4.16	5.42	−2.29	−2.81	4.12	−1.76	−1.60	3.28	−1.50	−0.66	2.17	−0.97	0.33*	0.41	0.12
0.4°	−3.68	7.39	−3.66	−1.65	6.36	−3.54	0.05	5.15	−3.15	3.30	3.12	−2.55	3.02*	2.58	−2.01	2.49*	1.81	−1.28			

[a] The phase shifts are nuclear phase shifts in degrees. Solution sets noted with an asterisk lie outside the solution region (Fig. 2) and do not give as good fits to the angular distribution as the sets lying within the solution region.

IX. ANALYSIS OF 31.8-MEV DATA

An inspection of the solution region for the 31.8-Mev Berkeley data[8] shown in Fig. 1 indicates that it does not appear to be consistent with the other data at higher and lower energies, being somewhat shifted in the direction of negative D-wave values. A phase-shift analysis of the data gives P waves that also correspond to a shift towards more negative D waves. The 31.8-Mev cross-section value at 90° shown in Table II agrees well with recent measurements at Minnesota.[19] If the angular distribution shown in Table II is altered by keeping the 90° value fixed, but raising the small angle values up by some 15% in a smooth fashion, the resulting phase shifts agree rather well with an extrapolation of the 20-Mev results. Table IX shows the effect of this change on the phase shifts.

At 40 Mev F waves are important, and the features of the S, P, and D waves at that energy have not yet been mapped out in a manner similar to the lower energy work. Hence it is not possible to say with certainty that the 31.8-Mev data are inconsistent with the other data. However, this appears to be the case. The data at 30.14 Mev[20] appear to have an even larger systematic error. The cross section at $\theta_{c.m.}=11°$, when compared with the data at 20 Mev and 40 Mev, seems to be low by perhaps 50%. It should be pointed out that the measurements at both 30.14 Mev and 31.8 Mev were made many years ago.

X. ANALYSIS OF 39.40-MEV DATA

At 40 Mev, F waves must be included in any analysis aimed at giving a good fit to the angular distribution. This greatly increases the multiplicity of possible solutions. Also no convenient parametrization method such as the Clementel-Villi method exists for F waves.

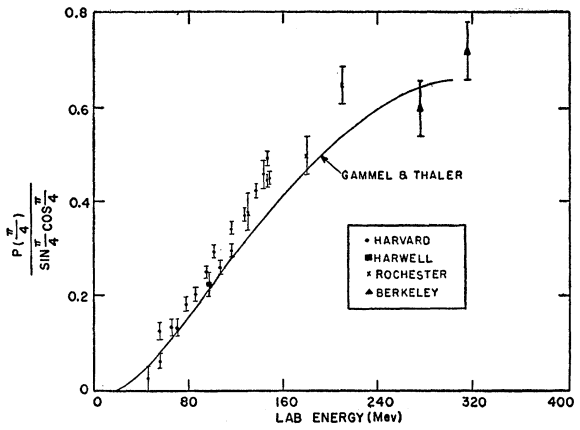

FIG. 6. Summary of p-p polarization measurements (reference 21) at $\theta_{c.m.}=45°$. The solid curve is the polarization predicted by the nuclear potential model calculations of Gammel and Thaler (reference 26).

[19] Y. S. Tsai and L. H. Johnston, Bull. Am. Phys. Soc. Ser. II, 3, 204 (1958).
[20] F. L. Fillmore, Phys. Rev. 83, 1252 (1951).

Angular distribution, polarization, and triple-scattering measurements are all essential in order to limit the multiplicity of solutions. The logical approach at the present time is to go up to an energy where these measurements do exist, determine the magnitudes of the F waves at that energy, and then extrapolate down in energy. Such a program is outside of the scope of the present paper. We shall limit ourselves here to showing that a solution does exist at 40 Mev that represents a reasonable extrapolation upward from the low-energy data.

The search code used in the present work includes the ${}^1S_0$, ${}^3P_0$, ${}^3P_1$, ${}^3P_2$, ${}^1D_2$, ϵ_2, and ${}^3F_2$ nuclear bar phase shifts, as defined by Stapp.[12] When S, P, and D phase shifts representing an extrapolation of a typical type I 20-Mev phase-shift solution set were used as the starting points for a search problem, with ϵ_2 and ${}^3F_2$ set initially at zero, the search ended with the following phase shifts: ${}^1S_0=40°$, ${}^3P_0=15.7°$, ${}^3P_1=-8.2°$, ${}^3P_2=3.8°$, ${}^1D_2=0.55°$, $\epsilon_2=-0.54°$, ${}^3F_2=1.41°$. This solution set gives a reasonable extrapolation of the S, P, and D waves, small but significant values for the F waves, and a polarization at 45° of about 1.5%, in agreement with experiment (Sec. XII). Other phase-shift solution sets at 40 Mev are given in reference 15.

XI. ESTIMATION OF THE ERRORS IN THE PHASE SHIFTS

The error matrix method[17] can be used to infer the uncertainties in the phase shifts. However, application of this method caused difficulties that are not completely understood. The ${}^3P_0$ phase shift has a much larger percentage error than any of the other phase shifts, and this may have been the cause of the trouble. The inverted error matrix was very sensitive to slight changes in the original matrix, and the diagonal elements of the error matrix were often negative. About all that can be said is that the uncertainty in ${}^3P_0$ is in general a few degrees for all solutions, and that the uncertainties in the other phase shifts are about a degree, with the ${}^1D_2$ phase shift being accurate to perhaps a tenth of a degree.

TABLE IX. S, P, D phase-shift solution sets at 31.8 Mev (${}^1S_0=45°$).[a]

Data as given in Table II				Data raised 15° at small angles			
${}^1D_2$	${}^3P_0$	${}^3P_1$	${}^3P_2$	${}^1D_2$	${}^3P_0$	${}^3P_1$	${}^3P_2$
			Solution I				
−0.2	3.85	−7.49	2.16	0.4	14.33	−7.02	0.90
0.2	−4.34	−6.80	3.03				
0.6	−7.73	−5.48	3.73	1.2	−10.7	−6.85	3.61
			Solution II				
−0.2	12.55	−3.21	−2.00	0.4	15.57	−6.09	−0.13
0.2	10.49	0.61	−4.31	0.8	17.30	−2.84	−2.53
0.6	7.94	3.58	−4.85	1.2	16.45	−0.24	−4.03

[a] Phase shifts in degrees.

TABLE X. Calculated double- and triple-scattering parameters at 18.2 Mev. The calculations correspond to the phase shift sets given in Table VII.[a]

C.m. scatt. angle (deg)	$^1S_0=50°$, Sol. I Values for $^1D_2$				$^1D_2=0.4°$, Sol. I Values for $^1S_0$				$^1S_0=50°$, $^1D_2=0.4°$ Solution types			
	0.2°	0.4°	0.6°	0.8°	49°	50°	51°	52°	I	II	III	IV
						$P(\theta)$						
15	−1.0	−0.6	−0.4	−0.2	−0.7	−0.6	−0.5	−0.3	−0.6	−1.4	−1.5	−0.7
30	−0.2	0.5	0.8	1.0	0.8	0.5	0.3	0.1	0.5	−1.2	−0.3	−1.2
45	0.4	1.0	1.1	1.3	1.4	1.0	0.7	0.3	1.0	−0.5	0.5	−0.9
60	0.5	0.9	0.9	1.1	1.2	0.9	0.6	0.3	0.9	−0.2	0.6	−0.7
75	0.3	0.5	0.5	0.6	0.7	0.5	0.3	0.2	0.5	−0.1	0.3	−0.4
						$D(\theta)$						
15	30	30	23	35	28	30	32	35	30	29	48	50
30	−34	−28	−23	−17	−31	−28	−25	−21	−28	−31	1	4
45	−21	−14	−9	−3	−17	−14	−12	−9	−14	−17	7	10
60	−16	−10	−3	3	−12	−10	−7	−5	−10	−11	6	7
75	−13	−7	−1	5	−9	−7	−6	−4	−7	−8	1	2
						$R(\theta)$						
15	29	30	33	34	28	30	32	34	30	28	48	50
30	−35	−31	−28	−24	−34	−31	−28	−23	−31	−32	3	11
45	−23	−22	−21	−18	−25	−22	−18	−15	−22	−17	11	23
60	−20	−22	−22	−21	−25	−22	−19	−15	−22	−12	11	29
75	−20	−25	−27	−26	−28	−25	−22	−18	−25	−9	9	31
						$A(\theta)$						
15	−3	−1	−0	0	−0	−1	−2	−3	−1	−6	−4	−8
30	12	5	0	−4	6	5	7	3	5	17	−6	7
45	13	1	−7	−13	1	1	−0	−1	1	22	−14	7
60	16	1	−8	−15	1	1	−0	−1	1	27	−18	4
75	20	4	−6	−13	5	4	3	1	4	32	−21	0
						$C_{kp}(\theta)$						
30	0.6	5.4	7.0	6.6	6.7	5.4	4.0	2.7	5.4	−5.5	−5.5	5.4
						$C_{nn}(\theta)$						
30	−78	−80	−82	−85	−75	−80	−85	−90	−80	−80	−71	−71

[a] The solution types are those listed in Table I. The scattering parameters are defined in reference 12, and the values are given in percent.

XII. DOUBLE- AND TRIPLE-SCATTERING EXPERIMENTS

In the preceding sections it was shown that there exists a multiplicity of phase shift solutions that give agreement with angular distribution measurements—a multiplicity that even very accurate angular distribution measurements would not remove. Polarization measurements can be used to remove some of the ambiguity. Unfortunately the smallness of the polarization below 40 Mev makes accurate measurements very difficult. Figure 6 summarizes the experimental p-p polarization measurements at a scattering angle of 45°. The lowest energy point is $P(45°)=1.25\pm1.25\%$ at 47 Mev.[21] These results indicate that the polarization below 40 Mev must be very small indeed. As a partial confirmation of the fact that the polarization continues to be small at low energies, Brockman[22] measured a polarization at 17.7 Mev of $-1.2\pm2\%$ at a c.m. scattering angle of 60°.

Table X summarizes the double- and triple-scattering parameters[12] that correspond to the phase shift solution sets given in Table VII. From Table X it can be seen that solution types I and III have positive nuclear ($\theta>30°$) polarizations, while II and IV have negative polarizations. An extrapolation of the high-energy polarization measurements indicates that at low energies the nuclear polarization is small and positive. Thus the ambiguity is reduced from four to two semi-infinite phase shift solution sets. The magnitude of the polarization at 18.2 Mev would of course provide additional information. However, it is shown in Table X that the magnitude is a function of both the S and D waves, and that the shape of the polarization curve as a function of angle is roughly the same for a range of S and D values. A polarization measurement at 18.2 Mev with an absolute accuracy of 0.1% at all angles would probably permit a choice between solution types I and III on the basis of the shape in the Coulomb interference region, but it would still leave a range of S–D combinations that would match both the angular distribution and polarization measurements.

Since the low-energy polarization is so small, as shown in Table X and Fig. 6, it seems worthwhile to investigate the triple-scattering parameters. Some of these parameters[12] are listed in Table X for the 18.2-Mev case. As can be seen, the parameters are rather

[21] This figure is from reference 16.
[22] K. W. Brockman, Jr., Phys. Rev. **110**, 163 (1958).

TABLE XI. Calculated polarizations at a center-of-mass scattering angle of 50 degrees.[a]

	Solution I			Solution II			Solution III		Solution IV	
				4.203 Mev						
S \ D	0	0.05	0.1	0	0.05	0.1	0.05		0.05	
51	0.13	0.20	0.29	−1.28	−1.49	−1.65	−0.67		−1.03	
53	−0.12	0.01	0.04	−0.32	−0.40	−0.27	−0.20		−0.21	
				9.68 Mev						
S \ D	0	0.1	0.2	0	0.1	0.2	0.1		0.1	
53	0.09	0.23	0.33	−0.80	−1.08	−1.27	−0.42		−0.89	
55	−0.06	−0.00	0.05	−0.24	−0.31	−0.23	−0.13		−0.16	
				18.2 Mev						
S \ D	0.2	0.4	0.6	0.2	0.4	0.6	0.4	0.6	0.4	0.6
49	0.86	1.33	1.45	0.73	−0.61	−1.28	0.72	1.44	−1.29	−1.41
51	0.24	0.61	0.53	0.26	−0.28	−0.78	0.37	0.87	−0.57	−0.69
53	−0.00	0.11	0.23	−0.01	−0.06	−0.21	0.10	0.24	−0.10	−0.21
				19.8 Mev						
S \ D	0.2	0.3	0.4	0.2	0.3	0.4	0.2	0.4	0.2	0.4
48	0.74	0.90	1.03	−0.90	−1.43	−2.04	−0.28	0.54	−1.39	−1.40
50	0.21	0.36	0.46	−0.65	−0.87	−1.01	−0.12	0.37	−0.58	−0.58
52	0.01	0.03	0.05	−0.07	−0.08	−0.09	−0.02	0.05	−0.04	−0.08

[a] Phase shifts in degrees; polarizations in percent. These calculations correspond to the phase-shift solution sets in Tables IV, VI–VIII.

large, so that triple-scattering experiments may be comparable in difficulty with polarization measurements at low energies. A measurement of $D(\theta)$ at a single angle, for example, would permit a choice between I–II and III–IV solution types. This measurement combined with a knowledge of the sign of the polarization would single out one solution type as the correct one. Just how many experiments would be necessary to assign precise values to S and D depends to a considerable extent on the accuracy of the measurements.

As a guide to experimenters planning to carry out polarization measurements, Table XI summarizes calculated polarizations at $\theta_{c.m.}=50°$ for phase-shift solution sets given in the preceding sections.

XIII. CALCULATION OF NUCLEAR PHASE SHIFTS IN BORN APPROXIMATION

In the preceding sections we have seen that angular distribution measurements can be fit by a multiplicity of phase-shift sets, and that polarization measurements only partly remove the ambiguity. Since no other experimental data exist in this energy region at the present time, the one remaining method of limiting the phase-shift sets is to calculate the phase shifts using a "reasonable" potential model. At the low energies considered here, the S phase shift is large, but the P and D phase shifts are small. Calculation of the S phase shift thus requires a knowledge of the potential in the vicinity of the repulsive core. But the P and D phase shifts, however, should be determined primarily by the outer part of the nuclear potential. In this and the following section, calculation of the small phase shifts only is attempted.

Since the P and D phase shifts are small, a Born approximation calculation was first carried out. Coulomb wave functions were used as eigenfunctions, and the nuclear potential was chosen to be the asymptotic second-order meson potential[23] extended to the origin. A difficulty arises in calculating the $^3P_2$ phase shift by this method, since the replacement of the tensor operator by "effective potentials" acting in each (J,l) eigenstate separately brings in off-diagonal contributions in this case (see the discussion of this point in the following section). However, the effect of these contributions can be estimated.

Evaluation of the Born approximation integral at a lab energy of 18.2 Mev gives the following phase shifts: $^3P_0=8.0°$, $^3P_1=-5.0°$, $^3P_2\simeq 1-2°$, $^1D_2=0.37°$. (These phase shifts will be compared with other calculations in the next section.) The asymptotic meson potential is only valid for distances of the order of 2×10^{-13} cm or greater.[24] Examination of the Born approximation integral shows that the contribution of the outer region ($r>2\times10^{-13}$ cm) is 0.7, 0.7, 0.5, and 0.98 of the total integral for the four phase shifts, respectively. Hence the outer region is quite important for the P waves and all-important for the D wave. Thus the use of the asymptotic meson potential all the way in to zero distance is probably not too bad for the P waves and seems justified for the D wave. A repulsive square-well core with a height of, say, 100 Bev and a radius of 0.5×10^{-13} cm produces a negligible change in the phase shifts.

Although the Born approximation seems accurate for

[23] Iwadare, Otsuki, Tamagaki, and Watari, Progr. Theoret. Phys. (Japan), Suppl. No. 3, 37 (1956).
[24] Reference 23, p. 36.

the D-wave calculation, it is apparent that the region near the core is of some importance for the P waves. The question arises as to what an infinite repulsive core would do to the phase shifts. In an answer to this question, the next section describes calculations made using the same nuclear potential but based on an integration of the radial wave equation rather than on the Born approximation.

XIV. CALCULATION OF NUCLEAR PHASE SHIFTS BY INTEGRATION OF THE RADIAL WAVE EQUATION

The nuclear potential chosen is the asymptotic second-order meson potential[23] combined with a repulsive core. Since the meson potential contains a tensor operator, mixing of the l-states occurs, and it is necessary to use coupled wave equations. However, as we restrict ourselves to the calculation of only P and D waves, the use of an uncoupled radial wave equation in each eigenstate separately leads to difficulty only for the $^3P_2$ phase shift, which couples to the $^3F_2$ phase shift. Using the WKB approximation, we can define an "effective potential" that will act only in the $^3P_2$ eigenstate,[25] and carry out the calculation with an uncoupled equation.

The core region was specified by a value for the core radius and a value for the logarithmic derivative (L_0) of the wave function at that radius. In this manner the sensitivity of the calculation to conditions near the core could be investigated. The integration was carried out by numerical iteration, using the Livermore Univac computer. At a sufficiently large value of r, the logarithmic derivative of the wave function was matched to Coulomb wave functions in a standard manner.

The results of calculations at 18.2 Mev are given in Table XII, which shows the dependence of the phase shifts on conditions at the core radius. For an infinite repulsive core ($L_0=\infty$), the calculated phase shifts are in good agreement with the Born approximation calculations of the preceding section. If the logarithmic derivative at the core is varied, however, the P phase shifts can assume any values, as shown in Table XII. The D phase shift is almost independent of conditions at the core, as is expected from the discussion in the preceding section. Since the Born approximation and infinite repulsive core calculations, which represent in a sense the two limiting cases of core potentials, are in agreement for the P phase shifts, it is tempting to say that these calculations are correct at least to the extent of giving the proper signs for the phase shifts.

TABLE XII. P- and D-wave phase shifts at 18.2 Mev as a function of the value of the logarithmic derivative at the core.

L_0[a]	$^3P_0$[b]	$^3P_1$	$^3P_2$	$^1D_2$
∞	10.15	−4.19	0.23	0.375
10	15.3	−4.11	0.68	0.377
4	50.5		1.13	
1	175.4	−3.98	2.06	0.380
−1	182.2	−3.90	6.16	0.381
−2			44.89	
−5.4		54.38		
−10	187.59	175.52	179.57	0.375
$-\infty$	190.15	175.81	180.23	0.375

[a] L_0 is the logarithmic derivative at a core radius of 0.58×10^{-13} cm.
[b] Phase shifts in degrees.

Calculations of phase shifts for an infinite repulsive core at several energies and for several core radii are given in Table XIII. Also included for comparison are the Born approximation calculations, and phase shifts calculated by Gammel and Thaler[26] and Signell and Marshak.[27] The agreement between the Gammel-Thaler phase shifts and the phase shifts calculated in the present work is very good, even though quite different potentials are used in the two models. The Signell-Marshak phase shifts are essentially n-p phase shifts since Coulomb effects were not included and should not be compared quantitatively with the other calculations shown. They do agree in sign and general magnitude

TABLE XIII. Phase shifts calculated from the asymptotic meson potential with an infinite repulsive core. Other calculations are also included for comparison.

Energy (Mev)	Core radius (in 10^{-13} cm)	$^1S_0$[a]	$^1D_2$	$^3P_0$	$^3P_1$	$^3P_2$	Comments
4.2	0.58		0.027	1.6	−0.8		Infinite repulsive core
9.7	0.48		0.14	5.7			Infinite repulsive core
	0.58		0.14	4.9	−2.2	0.2	Infinite repulsive core
	0.70			4.3		−0.03	Infinite repulsive core
18.2	0.48		0.38	12.5	−4.2	0.8	Infinite repulsive core
	0.58		0.38	10.2	−4.2	0.2	Infinite repulsive core
	0.70		0.37	8.4	−4.3	−0.1	Infinite repulsive core
19.8	0.58		0.42	11.1	−4.5	0.3	Infinite repulsive core
18.2			0.37	8.0	−5.0	1–2	Born approximation
10		54.3	0.09	5.6	−2.5	1.1	Gammel-Thaler[b]
20		49.2	0.37	10.1	−5.0	2.65	Gammel-Thaler[b]
18.2		51.4	0.2	3.1	−2.5	1.5	Signell-Marshak[c]

[a] Phase shifts in degrees.
[b] See reference 26.
[c] See reference 27.

[25] See, for example, J. S. Ball and G. F. Chew, Phys. Rev. **109**, 1385 (1958).
[26] J. L. Gammel and R. M. Thaler, Phys. Rev. **107**, 291 (1957).
[27] P. S. Signell and R. E. Marshak, Phys. Rev. **109**, 1229 (1958).

TABLE XIV. Type I phase shift solution sets for the D waves given in Table XIII.

$^1S_2$[a]	$^1D_2$	$^3P_0$	$^3P_1$	$^3P_2$	$P(50°)$[b]
		19.8 Mev			
48	0.42	2.84	−7.39	3.75	1.04
49	0.42	1.52	−6.40	3.44	0.73
50	0.42	−0.01	−5.20	3.07	0.47
51	0.42	−2.61	−3.33	2.54	0.26
		18.2 Mev			
48	0.38	9.43	−6.99	4.76	1.73
49	0.38	8.99	−6.12	4.49	1.33
50	0.38	8.01	−5.34	4.08	0.93
51	0.38	7.22	−4.34	3.68	0.60
52	0.38	6.04	−3.20	3.20	0.31
53	0.38	4.61	−1.62	2.55	0.10
		9.68 Mev			
54.0	0.14	3.83	−5.03	2.02	0.11
54.4	0.14	3.50	−4.50	1.80	0.06
54.8	0.14	2.77	−3.90	1.60	0.03
55.2	0.14	1.40	−3.19	1.44	0.02
55.6	0.14	0.07	−2.10	1.07	0.00
56.0	0.14	0.48	−0.94	0.40	−0.01
		4.203 Mev			
53.0	0.027	1.78	−3.35	1.56	−0.02
53.2	0.027	−1.00	−2.56	1.54	0.00
53.4	0.027	−2.06	−1.80	1.32	−0.01
53.6	0.027	−1.51	−1.40	1.04	−0.02
53.8	0.027	−0.82	−1.10	0.81	−0.02

[a] Phase shifts in degrees.
[b] Polarization in percent.

with the Gammel-Thaler and asymptotic meson potential calculations, giving P waves characteristic of solution type I.

XV. COMPARISON OF CALCULATED PHASE SHIFTS WITH EXPERIMENT

In the potential model calculations just discussed, the D-wave phase shift was found to be determined by the outer edge of the nuclear potential. Although some ambiguity arises in the calculation of the P waves, the models shown in Table XIII favor type I solution sets (we rule out type II by polarization arguments). With the point of view that the D wave is known from the model calculations and that the type I solution is the right one, a comparison between calculated phase shifts and experimentally-allowed phase shifts is given in Table XIV, using the D waves given in Table XIII. A comparison of Tables XIII and XIV shows that the agreement, while qualitatively good, is not precise enough to permit the determination of the S phase shift, for example.

It would be desirable to be able to say just what modifications in the nuclear potentials are required in order to fit the experimentally determined phase shifts within errors. However, such an undertaking should be attempted after enough experiments are available to permit the elimination of the phase shift multiplicity. Also, it is already clear that the meson-theoretic potentials give phase shifts that are in good qualitative agreement with the p-p experiments discussed in the present paper. To try to obtain precise quantitative agreement may mean that the static concept of the nuclear potential is being taken too seriously.[28]

XVI. CONCLUSIONS

The principal conclusion of the present work is that both polarization and triple-scattering experiments will be necessary in order to obtain an unique set of p-p phase shifts, even at low energies. Since the low energy polarizations are small and the low-energy triple-scattering parameters are large, the two types of experiments may well be of comparable difficulty.

At 1.8 Mev, the scattering is purely S wave within experimental errors. At 10 Mev, P- and D-wave effects are apparent. At 40 Mev, F waves are needed, even if the only criterion is a reasonable fit to the angular distribution data. The P-wave splitting in the S, P, D approximation is very sensitive to small changes in the S and D waves, and examination of Tables IV, VI–IX shows that the experimental angular distribution data are not all in agreement. Measurements at extremely small scattering angles are not particularly important with regard to nuclear phase shift determinations, since only Coulomb effects are being measured. More important are precise measurements of the shape and absolute magnitude of the cross sections. When considering effects such as vacuum polarization, the small-angle results are, of course, of considerable interest.

The rather extensive tables of phase-shift solution sets were included both because they serve to illustrate just what limitations are imposed by the existing experimental data, and because they are convenient starting points for future work.

ACKNOWLEDGMENTS

The author would like to thank Professor L. A. Johnston, Dr. D. E. Young, Professor J. R. Richardson, and Dr. D. J. Knecht for providing data prior to publication. Comments on this paper by a number of workers in the field were very helpful. The assistance of the Livermore computing staff, and in particular Mrs. H. Weber, is gratefully acknowledged. Special thanks are due to Professor G. F. Chew and Dr. H. P. Stapp for useful suggestions, and to Dr. H. P. Noyes who is responsible for many of the codes used in the present analysis.

[28] G. Breit, Phys. Rev. **111**, 652 (1958).